

SHOCK-BOUNDARY-LAYER INTERACTION IN FLIGHT

Arild Bertelrud
High Technology Corporation
Hampton, Virginia

SUMMARY

A brief survey is given on the study of transonic shock - boundary-layer effects in flight. Then the possibility of alleviating the adverse shock effects through passive shock control is discussed. A Swedish flight experiment on a swept wing attack aircraft is used to demonstrate how it is possible to reduce the extent of separated flow and increase the drag-rise Mach number significantly using a moderate amount of perforation of the surface.

BACKGROUND

The problem of shock-induced separation and associated buffeting became an important problem in aircraft development in the 1940s and the 1950s. Initially a large part of the investigations performed concerned flight tests, as it was a problem very much concerned with the direct flight application. Also, as long as the phenomenon was relatively unknown, it was not clear how much information the wind tunnel tests were able to give. Often observations in flight were verified in wind tunnels, and gradually it was possible to develop empirical relationships of use in the aircraft design.

Some of these early observations were of use much later. Notably, the aileron buzz phenomenon on the Lockheed F-80A airplane (Gadberg and Ziff, ref.1) was successfully computed by Steger and Bailey (ref.2) and Levy and Bailey (ref.3) with an unsteady, thin-layer Navier-Stokes code thirty years later.

For further information the reader is referred to Spreiter (ref.4) who has given an extensive historical survey concerning the early flight experiments and how they were correlated with theory and wind tunnel tests. Pearcey and Holder (ref.5) give an account of various investigations performed up to the mid-50s, including a variety of shock-modifying schemes.

Another period of intense effort also in flight testing was the discrepancy between tunnel predictions and flight reality experienced for the Lockheed C-141, where shock location in the wind tunnel case was 20% chord in front of the flight data (ref.6). A series of wind tunnel and flight experiments (ref.7) eventually led to improved methods of extrapolating the low Reynolds number wind tunnel data to higher Reynolds number flight data (Paterson et.al., ref.8); (Blackerby and Cahill, ref.9). In England (Browne et.al., ref.10) a VC-10 was instrumented with pressure tubing, and an extensive comparison was made between the full-scale flight results and data from a 1:15 model in a wind tunnel. Extensive work, was done in flight, as witnessed by the symposium on Supercritical Wing Technology (ref.11). The experimental information collected was compiled and resulted in empirical "rules of thumb" (ref.12) for

extrapolation of wind tunnel data to flight. In general the static pressure distribution at tunnel conditions (with appropriate interpretation as shock location etc.) was scaled through creation of empirical parameters. One recent investigation by Cunningham and Spragle (ref.13) uses more recent data for both two- and three-dimensional configurations.

Delery and Marvin (ref.14) have made an extensive review of shock-wave boundary-layer interactions (experiments as well as computational methods), and in the present conference, Ayers gives a paper on flight research and testing (ref.15).

Over the years a variety of drag-reducing techniques have been investigated for use in transonic flows. One method explored early on was introduction of vortex generators. Already in the early 1940s active control through suction and blowing on shock wave/boundary layer interaction was explored (refs.16-17). Krogmann (ref.18) has recently reviewed the subject area both regarding active and passive control, and only limited reference will therefore be given here to other work.

PASSIVE SHOCK CONTROL

While the active suction may give a gross drag reduction, the energy required for pumping may preclude a net gain. However, several authors have observed that even without pumping (passive control) there is often a drag reduction, i.e. a direct gain. Nagamatsu et.al. (ref.19) tested a 14 % thick supercritical NACA profile made porous from 53 to 85 % chord through use of a large number of holes. The result was slightly increased drag at lower Mach numbers while the drag-rise Mach number was increased. Krogmann et al. (refs.20-21) investigated the flow on another supercritical profile, the VA-2. Their perforation was obtained both through use of holes as well as single and double slots in the surface at selected positions. Again the drag-rise Mach number was increased; the buffet boundary was moved.

The assumption is that the passive shock control decreases drag through an automatic adjustment in the shock region. At the foot of the shock boundary layer air is pushed in through the perforations, while it is blown out further upstream where the pressure is low. Thus the maximum Mach number is reduced.

Figure 1 (ref. 18) illustrates the principle of this interaction and also introduces the coordinate systems and the definitions to be used. It appears that the main effect of the perforation is to allow a strong shock to be split into several weaker shocks, thus in some cases avoiding shock-induced separations. In two-dimensional flows it is possible to determine the overall effect on performance, and Figure 2 (Krogmann), shows the effect of passive ($C_q = 0$) and active shock control on the buffet boundaries of a supercritical profile. At least in this particular case, the main effect appears to be the surface perforation itself.

The size of the surface perforations relative to the local boundary layer thickness is important, as too large holes actually may cause a major disturbance through suction and blowing. Raghunathan and Mabey (ref.22) did an experiment on a 6% half circular arc airfoil to explore the effects of hole geometry; i.e. normal, forward- or backward facing holes. The forward-facing holes were found to give better results than the other. They also

investigated the effects of the perforation on the static pressure fluctuations. Savu (ref.23) did computations on the flow around a NACA 0012 profile with massive perforations, and conjectured the change in shock characteristics. Chen et.al.(ref.24) developed a full potential code to compute the flow over porous airfoils.

EXPERIMENT

Wind tunnel tests at transonic speeds are often cumbersome, as minor changes to a wind tunnel configuration easily may cause severe problems in the interpretation of data; both wall effects as well as free stream turbulence and disturbances tend to cause problems. Also, the added complication of manufacturing porous surfaces for small wind tunnel models, make wind tunnel tests of passive shock control hard. Computational tools under development often need good experimental data for comparison, and to avoid all uncertainties due to the wind tunnel environment, flight data has been utilized as a database in the present study.

The experiment was performed on a swept wing attack aircraft (ref.25), a SAAB 32A Lansen, and the results are available as a computerized database (refs.26-27) allowing a comprehensive description of aerodynamic flow on a swept wing in the entire subsonic flight regime. Figure 3 shows the geometry of the aircraft and the flight envelope while Figure 4 yields the wing geometry and coordinate systems.

The wing geometry was used as baseline for a series of transonic wings developed at the FFA in the 1970s - extensive studies of the force and moment characteristics as well as pressure distributions with a scale model at high Reynolds numbers were made.

INSTRUMENTATION AND EXPERIMENTAL SETUP

Comprehensive transonic measurements in flight require ample flight time, good description of reference conditions and a well organized data handling system. It is in general necessary to perform the measurements with only a few probes per flight to make sure that the shock pattern stays the same. One of the experiences using glued on tubing for pressure distributions in the VC-10 experiment was that the tubing indicated the correct pressure, but the value and the flow field were affected by the tube presence. In the present experiment the transonic flow mapping was performed over a large portion of the test, adding information a small piece at a time. In Figure 5, the sensor types used have been indicated. The modular approach, allows sensor complement, location and type to vary from flight to flight; as has been done recently on a Boeing 737 (ref.28). The validity of one sensor type often requires information obtained with another type of sensor. For example the static pressure measured with the modified Preston tube (refs.29-30) must be compared with the wall pressure taps at some locations. Also the cross-flow must be small, which requires information from dual hot films. These in turn require information on the static pressure for a proper evaluation. The solution to this apparent maze is use of redundant data and an efficient data handling system that solve most of the interrelations automatically. In general each aerodynamic parameter should be measured with at least two methods.

Another problem is the choice and repeatability of flight conditions. The ability to keep Mach number constant and have minimized control surface deflections while also keeping altitude requires a lot from pilot and aircraft. Also the weight of the aircraft and its trim should ideally be repeatable from flight to flight, to ensure the same angle of attack. The weather varies, both the turbulence characteristics and parameters like temperature and humidity.

The wing was equipped with a large number of static pressure taps - mostly in the leading-edge region (ref. 24), but the distributions of pressure and local skin friction were also determined using modified Preston tubes.

This gave a coarse grid information in the chordwise as well as spanwise direction also as the Mach number increased, although the chordwise resolution was insufficient for proper shock documentation.

The main source of information used in the present study on shock/boundary-layer interaction is 51 static pressure taps close to the wing tip - see Figure 4. This row covers the region from $\xi = 0.2$ to the trailing edge, and is supplemented by 13 static pressure taps in the leading-edge region. The pressure taps are located in a plane intersecting the leading edge at $\eta = 0.912$ and the trailing edge at $\eta = 0.812$, being the non-dimensional spanwise location.

From previous experience it is known that the shock is located somewhere between $\xi = 0.4$ and 0.6 depending on the flight altitude, and the pressure taps were positioned accordingly. To monitor spanwise variations two additional rows of pressure taps, inboard and outboard, were used in the shock region itself.

It is very hard to document whether or not flow is separated using only the static pressure as an indicator, and in the present study a three-step technique was employed:

- During one flight the row of pressure taps was used uncovered, to document C_p .
- During a second flight some of the taps were covered by razor blades with the edge pointing forward; acting as Stanton tubes.
- During a third flight some of the pressure taps were covered by razor blades facing backwards, acting similar to Stanton tubes and intended to detect backflow.

Figure 6 shows boundary-layer development in front of the shock. At $\xi = 0.6$ a pressure rake was positioned, aligned with the flight direction. In most cases a limited shock-induced separation would be located close to $\xi = 0.6$, and it was considered important to have viscous layer information as far back as possible. Both total pressure and Mach number profiles were monitored; the wall static pressure was normally used for evaluation of integral properties but the static pressure 30 mm from the wall was also measured.

In the interaction region this may be questionable, but as the purpose of the investigation is to explore possible effects of

surface perforation, useful comparisons can be made. To verify whether or not the flow is separated is also a difficult task with the pressure rake data, and for this purpose extra flights were made with Stanton tubes (razor blades) over some of the pressure taps. Local skin friction may be determined if a universal calibration law is assumed valid.

One heated dual wall film probe was located in the shock region to monitor flow angularity and turbulence, but the data have not been evaluated so far.

The surface perforation was located at $\xi = 0.42$ and $\xi = 0.58$ respectively, as can be seen in Figure 4. They consisted of 2 and 3 mm diameter holes with a spacing of 15 mm; this is equivalent to the perforation used by Krogmann et.al.(ref.20). In the figure the various configurations used are defined ranging from 0 to 3.14 % porosity. The cavity used in this case was a reasonably well sealed box in the wing structure, extending from the front to the rear beam. Cavity pressure was monitored using five static pressure taps on the cavity walls.

FLOW CONDITIONS

Two flight altitudes were used for the flight experiments, 7 and 10 km, and Figure 7 may serve to illustrate the type of results obtained. At the same Mach number, the shock is moved forward roughly 3% chord due to changes in altitude. From the Figure it is clear that a high resolution is needed to find the pressure gradient in the pressure-rise region and to monitor the separation bubble beneath/behind.

One parameter used when comparing 2D and 3D flows at transonic Mach numbers is the Mach number component normal to the shock, M_{LN} . It plays a dominant role when predicting separation limits. In the present case the three-dimensional shock pattern is not well defined in the spanwise direction. In fact, shock splitting etc. may occur, and therefore the experimental results have been evaluated using the Mach number normal to the local surface generator. Using the measured pressure coefficient, the Mach number component normal to the generator may be determined (comparable to a 2D flow) to find at what flight Mach number there is a possibility of a shock. Figure 8 shows the peak Mach number normal to the local generator, P_{MLN} , as a function of flight Mach number for one choice of perforation. As can be seen only $M > 0.87$ should be of interest in the present case. It can also be noted that shock-induced separation occurs at $M = 0.895$ for $H = 10 \text{ km}$ and $M = 0.905$ at $H = 7 \text{ km}$ for the present perforation. This figure may also serve to illustrate the repeatability of the data.

A note of caution is needed before discussing the general results from the tests. In a three-dimensional case of shock wave/boundary layer interaction almost any combination of flow pattern is possible, hysteresis, unsteadiness as well as interference from probes may actually dominate the flow, and Figure 9 may be used as a reminder of this. During nominally stationary conditions, the pilots of the

present tests are required to maintain an indicated speed and altitude. As a consequence of reasonable tolerances in these two parameters, the Mach number may vary. This does not normally create any problems, but in the present Figure an increase in flight Mach numbers of 0.005 has caused the flow to separate, causing a drop in the pressure coefficient upstream of the shock. The total pressure coefficients as well as the indicated Mach number profiles at $\xi = 0.6$ are drastically changed, and the main question to ask in this case is whether or not the changes observed are typical of the corresponding Mach numbers.

The figure also demonstrates the difficulty of determining a proper Mach number profile from total pressure measurements, as the static pressure chosen for the data reduction may seriously affect the result. In this paper the value obtained from a wall pressure tap is used throughout the viscous layer. Also, as backflow cannot be measured, it is not reasonable to include the separated region in the integration of displacement and momentum thicknesses if the flow is separated, and this should be borne in mind when local values of δ^* , θ and H are examined.

As the Mach number increases, the shock starts to grow in strength and moves back on the wing - as illustrated in Figure 10, where shock position is plotted against PMLN. Two positions are indicated for each case; location of the peak Mach number and the location of the sonic line. The movement is roughly 10% chord as the shock grows and separation occurs, and the rear region of ventilation holes close to $\xi = 0.58$ is behind the sonic line for the attached case, in front of it for the separated.

Figure 11 may illustrate the boundary layer behind the shock location as function of the peak normal Mach number. The pressure rake was located at $\xi = 0.6$, and the momentum thickness is seen to increase dramatically. Also the shape factor H increases to around 3 before separation. For separated flow it was not possible to obtain information on the reversed flow, and thus the filled symbols of the figure are based on integration out from the zero-velocity point. As can be seen this agrees quite well with the decrease in peak Mach number due to separation. However, it means that the very high values of H sometimes associated with the shock-induced separation are not given here.

To evaluate the drag-reducing characteristics of the perforated surfaces, it was necessary to measure the boundary-layer characteristics downstream of the separated region. This was done for the following configurations:

PERFORATION		
Notation	$\xi = 0.42$	$\xi = 0.58$
OPEN	3.1 %	3.1 %
CLOSED/OPEN	0 %	3.1 %
CLOSED/BASELINE	0 %	0 %

In Figure 11 a distinction is made between points with or without separation further forward using filled and open symbols respectively. There is a clear indication that the increase in H is delayed to higher flight Mach numbers, and also that the separation itself is delayed. However, Figure 11 does not contain the full story on drag effects - the static pressure may have changed in some cases.

Therefore the data were transferred to far-wake conditions using Squire-Young's formula, and the result is plotted in Figure 12. Here the configuration with perforation at the shock itself (i.e. normal blowing) is seen to delay drag-rise substantially, from $M = 0.88$ to 0.92 for this span station, which is the most critical one. At lower Mach numbers the drag is not affected significantly by the downstream perforation, whereas also having upstream perforation appears to increase drag irrespectively of flight Mach number.

CONCLUSIONS

Passive shock control through surface perforation:

- It is possible to decrease drag through local perforation in the order of 2 % over a limited region at the shock. The gain is evident in a limited Mach number region only, and hence the wind tunnel data suggesting a shift in divergence Mach number appears appropriate.
- Perforating the surface far in front of the shock had negative effects, thus increasing drag without beneficial effects concerning the divergence Mach number. This is in agreement with Nagamatsu et. al.; although the shock may be weakened, the added boundary-layer flow upstream may have detrimental effects. In the present case it is probable that the large perforation size (compared to the boundary layer thickness) had a considerable effect.

REFERENCES

1. Gadberg,B.L. and Ziff,H.L.: "Flight Determined Buffet Boundaries of Ten Airplanes and Comparisons with Five Buffeting Criteria." NACA RM A50127 (1951).
2. Steger,J.L. and Bailey,H.E.: "Calculation of Transonic Aileron Buzz." AIAA Paper 79-0134 , Jan. 1979.
3. Levy,Jr,L.L. and Bailey, H.E.: "Computation of Airfoil Buffet Boundaries." AIAA Journal, Vol 19, No 11, 1981, pp. 1488-90.
4. Spreiter,J.R. " Transonic Aerodynamics - History and Statement of the Problem." in Nixon,D. (Ed.) " Transonic Aerodynamics." Vol. 81, Progress in Astronautics and Aeronautics, AIAA, 1982.

5. Pearcey, H.H. and Holder, D.W.: "Examples of the Effects of Shock-Induced Boundary-Layer Separation in Transonic Flight." ARC R&M 3510 (1967).
6. Loving, D.L.: "Wind-Tunnel - Flight Correlation of Shock-Induced Separated Flow." NASA TN D-3580, 1966.
7. Blackwell, J.A., Jr.: "Preliminary Study of Effects of Reynolds Number and Boundary-Layer Transition Location on Shock-Induced Separation." NASA TN D-5003, 1969.
8. Paterson, J.H., Blackerby, W.T., Schwanebeck, J.C. and Braddock, W.F.: "An Analysis of Flight Test Data on the C-141A Aircraft." NASA CR-1558, 1970.
9. Blackerby, W.T. and Cahill, J.F.: "High Reynolds Number Tests of a C-141A Aircraft Semispan Model to Investigate Shock-Induced Separation." NASA CR-2604, 1975.10. Anonymous : "Supercritical Wing Technology - A Progress Report on Flight Evaluations." NASA SP-301, 1972.
10. Browne, G.C., Bateman, T.E.B., Pavitt, M. and Haines, A.B.: "A Comparison of Wing Pressure Distributions Measured in Flight and on a Windtunnel Model of the Super V.C.10. ARC R&M 3707, 1972.
11. Palmer, W.E. and Elliott, D.W.: "Summary of T-2C Supercritical Wing Program." in NASA SP-301, 1972.
12. Cahill, J.F. and Connor, P.C.: "Correlation of Data Related to Shock-Induced Trailing-Edge Separation and Extrapolation to Flight Reynolds Number. NASA CR-3178, September 1979.
13. Cunningham Jr., A.M. and Spragle, G.S.: "A Study of the Effects of Reynolds Number and Mach Number on Constant Pressure Coefficient Jump for Shock-Induced Trailing-Edge Separation. NASA CR-4090, August 1987.
14. Delery, J. and Marvin, J.G.: "Shock-Wave Boundary-Layer Interactions". AGARD AG-280 (1986).
15. Ayers, T.G.: "Flight Research and Testing." Transonic Symposium - Theory, Application, and Experiment., NASA Langley Research Center, Hampton, Virginia, April 19-21, 1988.
16. Regenscheit, B.: "Versuche zur Widerstandsverringerung eines Flügels bei hoher Mach'scher Zahl durch Absaugung der hinter dem Gebiet unstetiger Verdichtung abgelösten Grenzschicht." ZWB-FB-1424, Juli 1941, english translation : NACA TM 1168, July 1947.
17. Page, A. and Sargent, R.F.: "Effect on Airfoil Drag of Boundary Layer Suction Behind a Shock Wave." ARC R&M 1913, 1943.

18. Stanewsky, E. and Krogmann, P.: "Transonic Drag Rise and Drag Reduction by Active/Passive Boundary Layer Control". VKI Lecture Series "Aircraft Drag Prediction and Reduction", May 1985. (AGARD-R-723).
19. Nagamatsu, H.T., Dyer, R. and Ficarra, R.V.: "Supercritical Airfoil Drag Reduction by Passive Shock Wave/Boundary Layer Control in the Mach Number Range 0.75 to 0.90." AIAA Paper 85-0207.
20. Krogmann, P., Stanewsky, E. and Thiede, P.: "Effects of Local Boundary Layer Suction on Shock-Boundary Layer Interaction and Shock-Induced Separation." AIAA Paper 84-0098, AIAA 22nd Aerospace Sciences Meeting, Reno, Nevada, January 9-12, 1984.
21. Krogmann, P. and Thiede, P.: "Aktive und Passive Beeinflussung der Stoss-Grenzschicht-Interferenz an Überkritischer Tragflügeln." DFVLR IB 222 83 A 26 , October 1983.
22. Raghunathan, S. and Mabey, D.G.: "Passive Shock-Wave/Boundary-Layer Control on a Wall-Mounted Model." AIAA Journal, Vol 25, No 2, February 1987, pp. 275-278.
23. Savu, G. and Trifu, O.: "Porous Airfoils in Transonic Flows." AIAA Journal, Vol. 22, No. 7, July 1984, pp.989-991.
24. Chen, C.L., Chow, C.Y., Holst, T.L. and Van Dalsem, W.R.: "Numerical Simulation of Transonic Flow Over Porous Airfoils."
25. Bertelrud, A.: "The Role of Free Flight Experiments in the Study of Three-Dimensional Shear Layers". presented at "Perspectives in Turbulence Studies", International Symposium dedicated to the 75th Birthday of J.C. Rotta, Gottingen, May 11-12, 1987.
26. Bertelrud, A. and Olsson, J.: "Method of Analysing Data on a Swept Wing Aircraft in Flight." ICAS Paper 86-1.9.3 in ICAS Proceedings 1986, 15th ICAS Congress, London, September 1986.
27. Bertelrud, A.: "Pressure Distribution on a Swept Wing Aircraft in Flight." in AGARD AR-138 Addendum. (1984).
28. Bertelrud, A., Boeck, J., Heaphy, W. & Parks, M.: "A Real-Time Aerodynamic Analysis System for Use in Flight. "AIAA Paper 88-2128, 4th Flight Test Conference, San Diego, May 1988.
29. Preston, J.H. "The Determination of Turbulent Skin Friction by Means of Pitot Tubes." J. Aeron. Soc., Vol. 58, pp. 108-121 (1954).
30. Bertelrud, A.: "Total Head/Static Measurements of Skin Friction and Surface Pressure. "AIAA Journal, Vol. 15, March 1977, pp. 436-438.

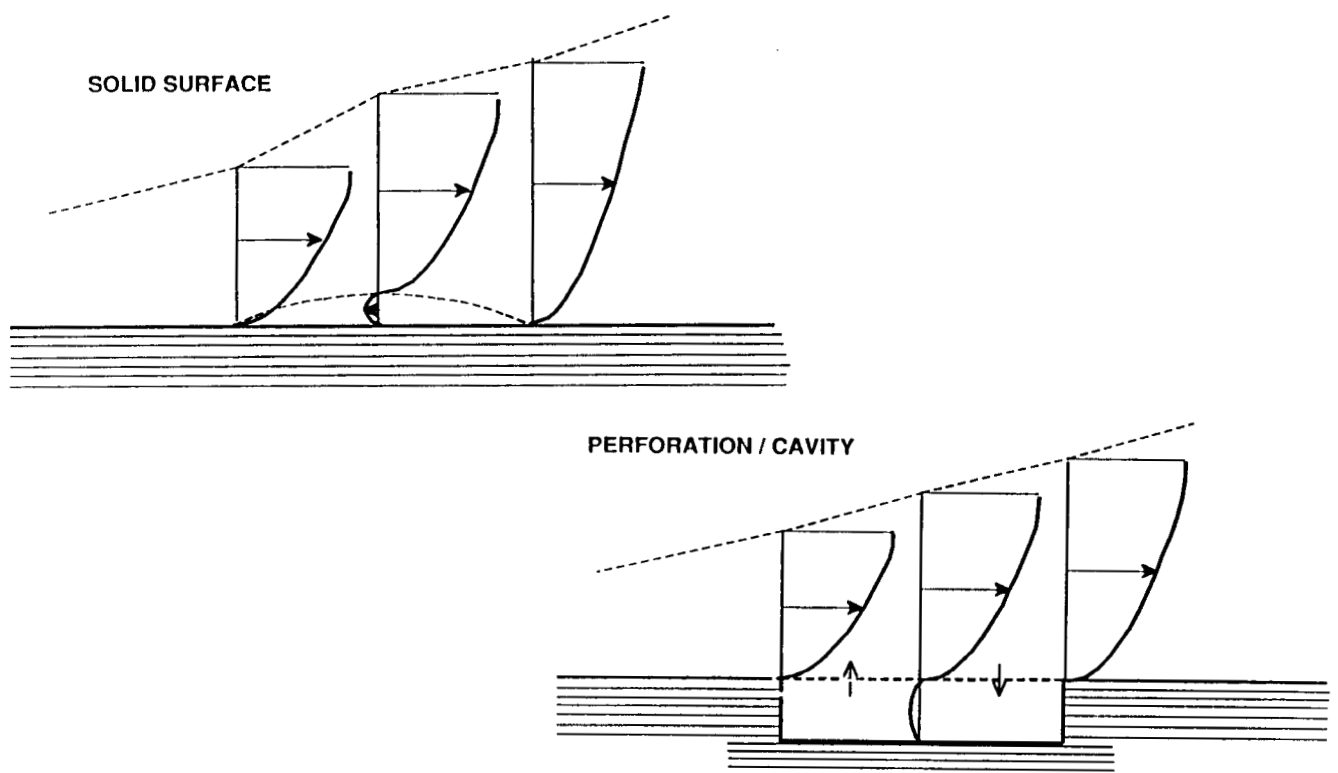


Figure 1 Principle of passive shock control (From ref. 18)

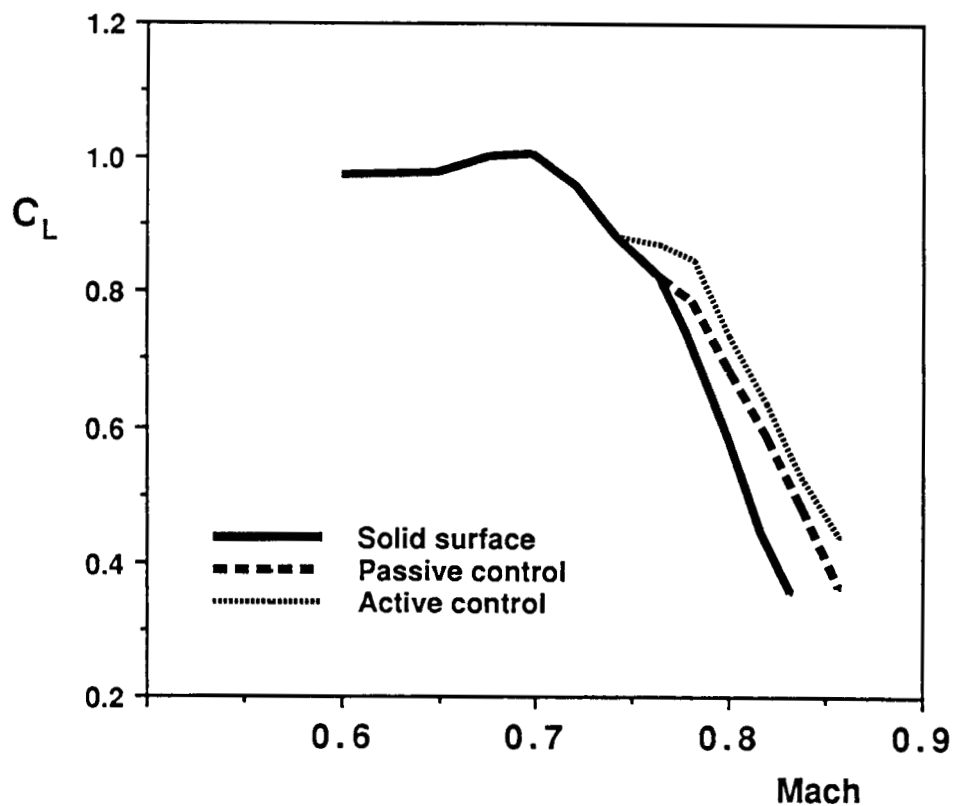


Figure 2 Effect of passive shock control on buffet boundary (From 18.)

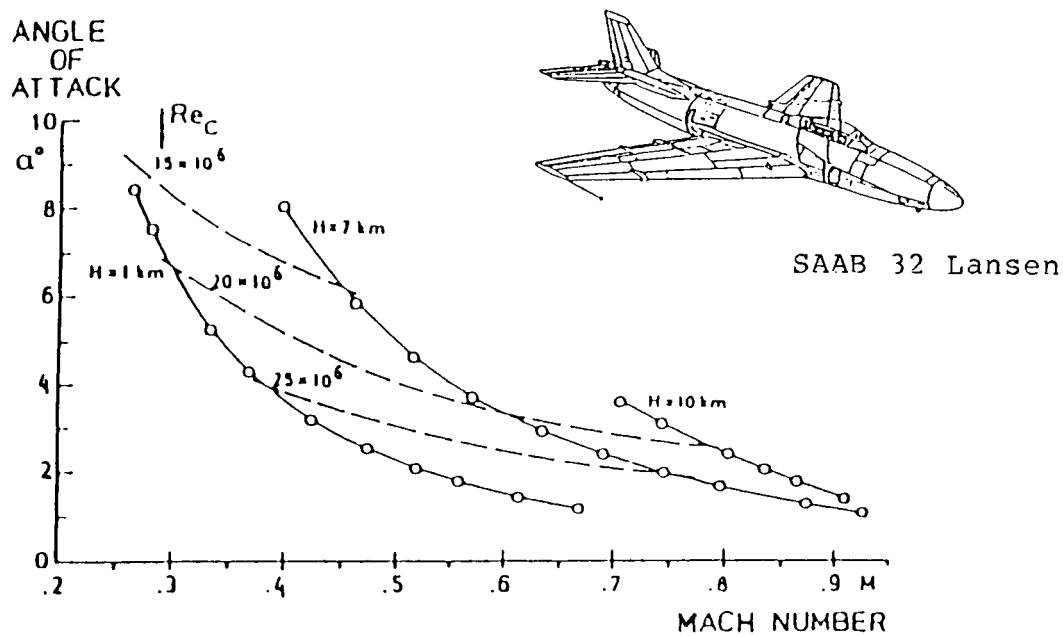


Figure 3 Geometry of the aircraft and the flight envelope.

TEST AREA ON THE OUTER PART OF THE WING

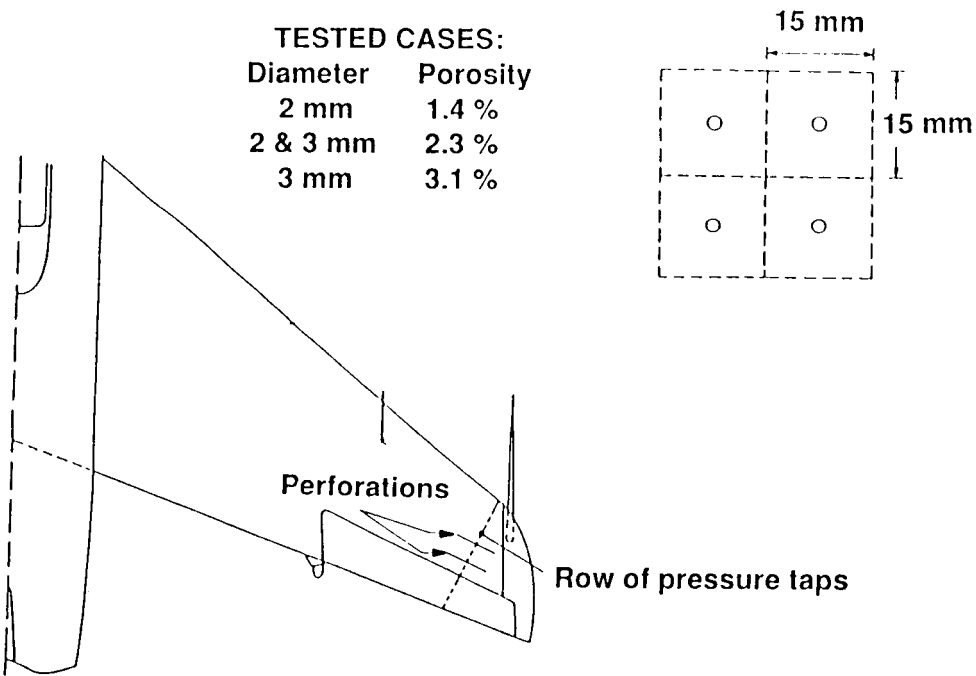


Figure 4 Wing geometry and coordinate system.

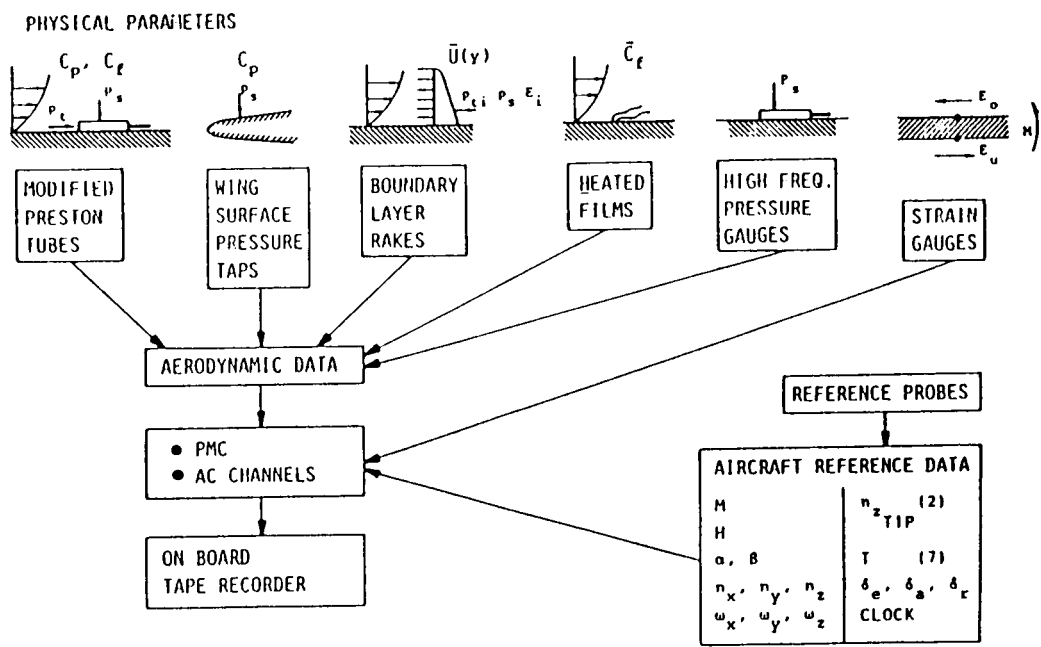
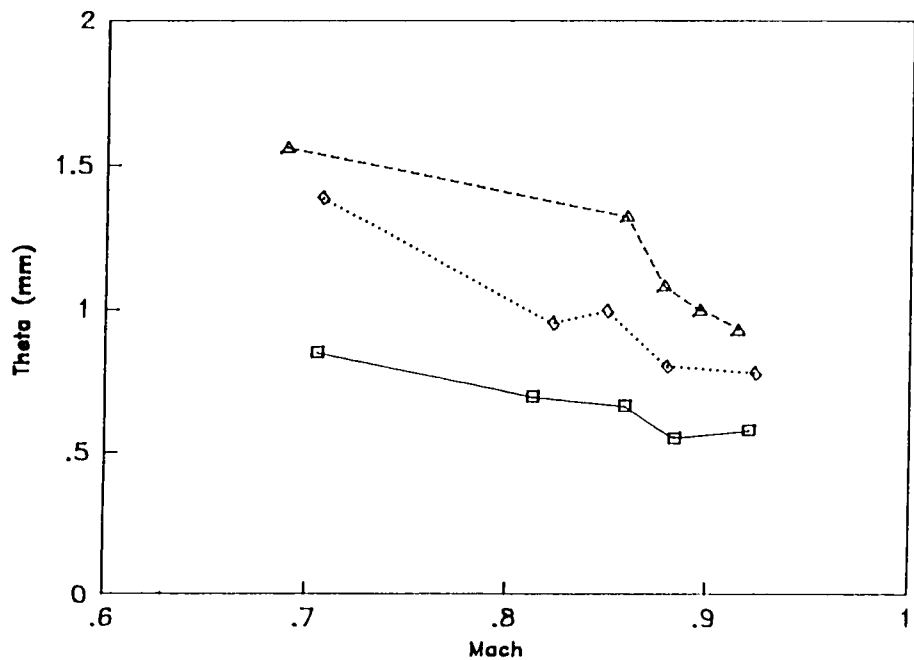


Figure 5 Sensor types and data acquisition system.

BL AT 20,30 & 40 % CHORD



BL AT 20,30 & 40 % CHORD

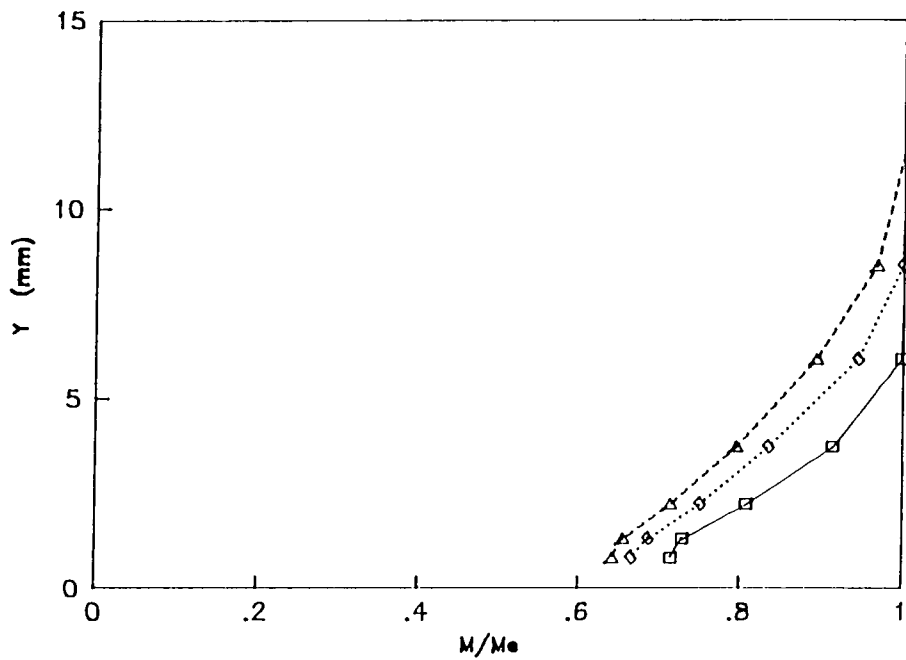


Figure 6 Boundary layer development in front of the shock. Baseline.

SHOCK POSITION AT CONSTANT MACH NUMBER BASELINE

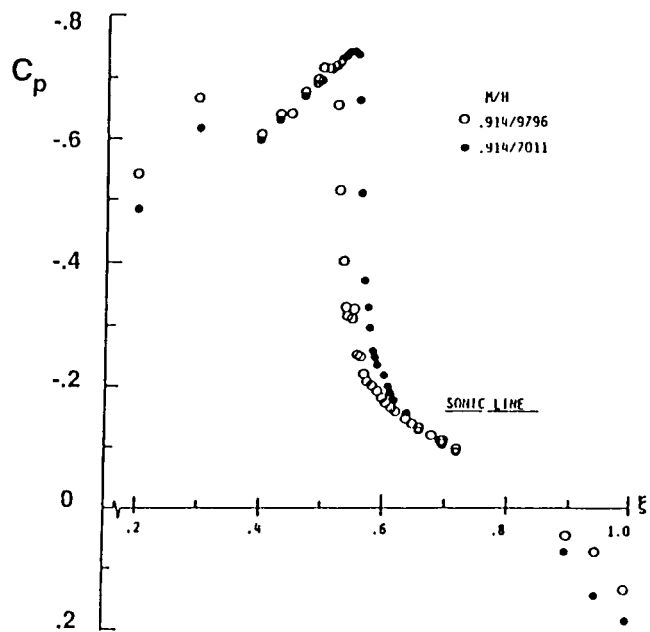


Figure 7 Shock movement due to change in altitude, baseline.

PEAK NORMAL LOCAL MACH NUMBER (PMLN) 1.4 % POROSITY

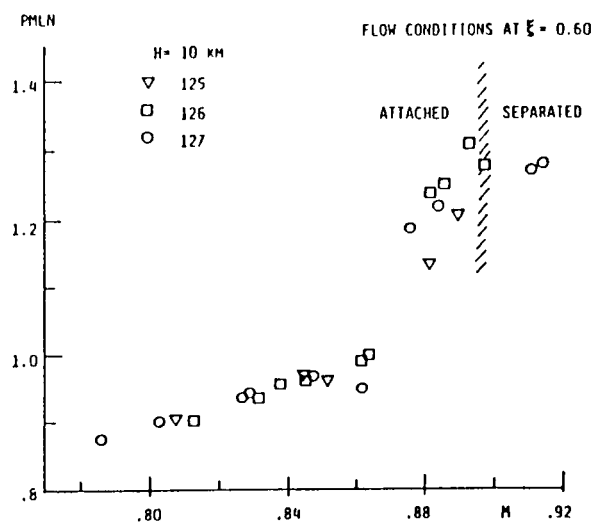


Figure 8 PMLN as function of flight Mach number.

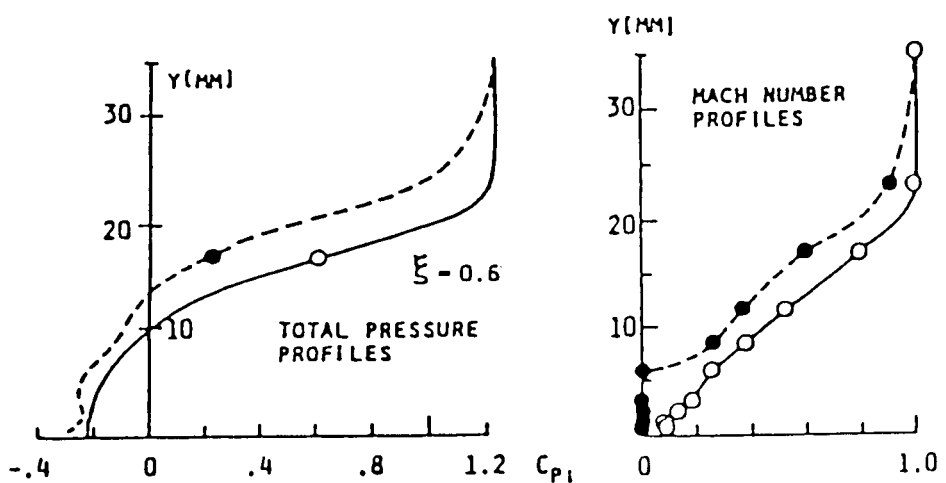
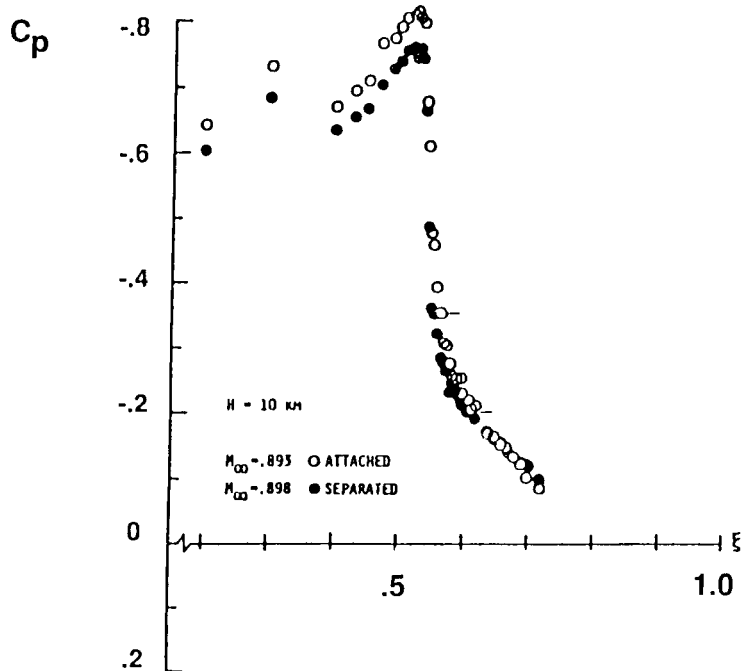


Figure 9 Flip-flop effect of separation, baseline.

SHOCK POSITION AT CONSTANT ALTITUDE BASELINE

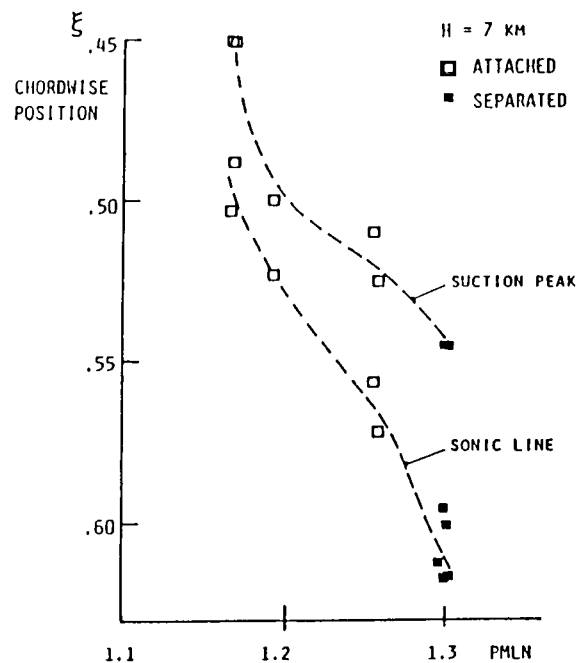


Figure 10 Shock movement due to changes in Mach number, baseline.

BOUNDARY LAYER PARAMETERS AT 60 % CHORD 3.1 % POROSITY

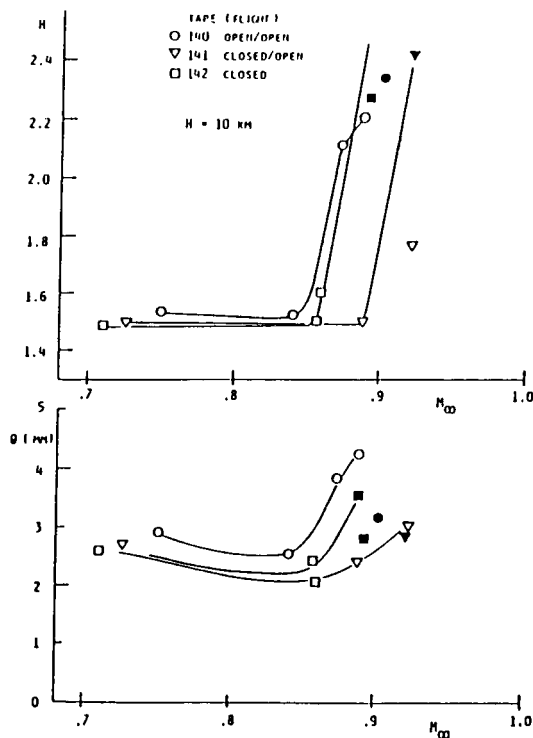


Figure 11 Momentum thickness and shape factor as function of PMLN at 60 % chord.

MOMENTUM LOSS - DOWNSTREAM EFFECT 3.1 % POROSITY

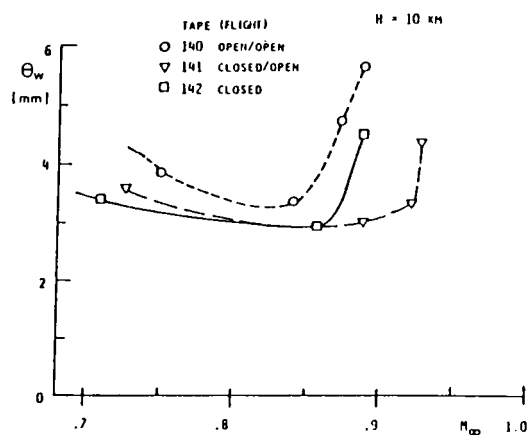


Figure 12 Momentum deficit interpreted as drag using the Squire-Young formula.